frontiers | Frontiers in Environmental Science

TYPE Original Research
PUBLISHED 25 January 2023
DOI 10.3389/fenvs.2023.1106181

OPEN ACCESS

EDITED BY
Biyun Guo,
Zhejiang Ocean University, China

REVIEWED BY
Shuo Zhang,
Tsinghua University, China
Xuefei Chen,
Guangzhou Institute of Geochemistry (CAS), China

*CORRESPONDENCE
Binkai Li,
libk@isl.ac.cn

SPECIALTY SECTION
This article was submitted to Freshwater Science, a section of the journal Frontiers in Environmental Science

RECEIVED 23 November 2022
ACCEPTED 11 January 2023
PUBLISHED 25 January 2023

CITATION
Ren Q, Li B, Zhang Y and Wu H (2023), Origin and evolution of intercrystalline brine in the northern Qaidam Basin based on hydrochemistry and stable isotopes. *Front. Environ. Sci.* 11:1106181. doi: 10.3389/fenvs.2023.1106181

Origin and evolution of intercrystalline brine in the northern Qaidam Basin based on hydrochemistry and stable isotopes

Qianhui Ren[1,2,3], Binkai Li[4]*, Yan Zhang[5] and Haitao Wu[1,2,3]

[1]School of Water Resources and Electric Power, Qinghai University, Xining, China, [2]Laboratory of Ecological Protection and High-Quality Development in the Upper Yellow River, Xining, China, [3]Key Laboratory of Water Ecology Remediation and Protection at Headwater Regions of Big Rivers, Ministry of Water Resources, Xining, China, [4]Qinghai Institute of Salt Lakes, Chinese Academy of Sciences, Xining, China, [5]The Third Qinghai Nonferrous Metals Geological Exploration Institute, Xining, China

The Kunteyi Basin, located in northern Qaidam, is known as a significant potash ore deposit in China. It is of great significance to study the origin of the potassium-rich intercrystalline brine to support the exploitation of potassium salts. In this study, the major ion concentrations and isotopic ratios (δ^2H, $\delta^{18}O$, and $\delta^{11}B$) of intercrystalline brine were used to analyze the evolution of the brine. The results show that the intercrystalline brine has a much higher concentration of total dissolved solids compared with the oil-field brine. Most of the ions are enriched except Ca^{2+} and Br^-. The value of δ^2H and $\delta^{18}O$ are much negative while the $\delta^{11}B$ values are positive. The analysis of C_{Na}/C_{Cl}, C_{Br}/C_{Cl}, Cl/(Na + K + Mg) and isotopes ratios, indicate that (1) Atmospheric precipitation is the primary source of water in brine; (2) The salinity of the brine is mainly influenced by halite dissolution; (3) The study area was influenced by the deep hydrothermal fluids. The thermal water recharged the Pleistocene layer, reacted with polyhalite, and formed Mg- and K-rich brine. The solution rose along the channel formed by the Shuangqiquan Fault and was supplied to the shallow intercrystalline brine.

KEYWORDS

Qaidam Basin, Kunteyi Playa, intercrystalline brine, origination, isotopes

1 Introduction

The origin of brines in the sedimentary basin has a significant implication for understanding the processes of water migration, sedimentary deposition, salt separation, and variation of paleoclimates (Farber et al., 2007; Bershaw et al., 2012; Ye et al., 2015; Basyoni and Aref, 2016). Two questions need to be answered to identify the brine origin, i.e., where the water comes from and how salinity enriches (Bagheri et al., 2014). Two main hypotheses answer the first question. One suggestion is that water came from the residual paleo-seawater, whereas others have suggested the influence of meteoric water and mantle water. The source of salinity in the brine is more complex than that of the proposed origin waters. It can be transformed by many factors, such as seawater concentration, sedimentary weathering or dissolution, and thermal water supply. However, under evaporation and salt crystallization, brines of different origins have similar chemical compositions and associated minerals (Vengosh et al., 1995), which complicates research on brine evolution.

The Qaidam Basin, a Cenozoic sedimentary basin, is a typical interior basin. There are dozens of different sizes of salt lakes, salinas, and playas in the Qaidam Basin. The

sedimentary sequence and tectonic deformation of the Qaidam Basin have recorded the evolution and growth history of the Tibetan Plateau since the Indian–Eurasian plate collision (Yin and Harrison, 2000; Tapponnier et al., 2001; Royden et al., 2008). Under the influence of deep water, volcanic hydrothermal water, and the surrounding rock, the brines of different locations have different hydrochemical characteristics and sources (Ye et al., 2015). In addition, many mineral resources, such as petroleum, potassium, boron, and strontium, exceed the Chinese industrial grade (Tan et al., 2011). Brine is a special kind of water with a total dissolved solid (TDS) content greater than 50 g/L. The intercrystalline brine indicates that the brine remains in the pore structure of the stratum and has undergone a similar evolution process as the formation of minerals. Therefore, research on the origin of brine also helps in understanding the process of mineral formation and improves the efficiency of mineral exploitation.

As playas and hypersaline lakes account for one-quarter of the Qaidam Basin, the origin of these brines has attracted considerable attention (Yu et al., 2013). These researchers agree on two evolutionary mechanisms, i.e., evaporation and dissolution. Analyzing the ion content and isotopic compositions of $\delta^{18}O$, $\delta^{2}H$, and $\delta^{37}Cl$, Du et al. (2016) suggested that the shallow brine of the Qaidam Basin originated from evaporation and was influenced by rainwater that dissolved halite. However, sources of water and salinity are highly controversial. For example, the $\delta^{18}O$ and $\delta^{2}H$ values of brines in the Qaidam Basin, near the meteoric water line, indicate that the brine originated from paleo-meteoric water (Fan et al., 2010; Han et al., 2013; Ye et al., 2015). However, based on the tectonic movement of the Tibetan Plateau, Li et al. (2013b) explained the high $\delta^{11}B$ value of brines in Xiaoliangshan using modified paleo-seawater. In addition, the chemical composition and elemental ratios indicated the influence of thermal water or magmatic fluids. In general, most researchers agree that the evolution of brines is associated with non-marine evaporation. However, these studies did not discuss the origin of water and salinity separately and there is still doubt regarding brine circulation in different regions and depths.

The study area, Kunteyi Salt Lake, located in the western Qaidam Basin, is a vital potash ore deposit containing several Cenozoic brines. In this study, we used $\delta^{18}O$, $\delta^{2}H$, and $\delta^{11}B$ isotopes and ion chemistry to explain the origin of the brine. Traditional elemental geochemical analysis methods have been used to study brine sources. The application of conventional and non-conventional isotope methods makes brine source research more accurate (Vengosh et al., 1995). In this method, we attempt to understand water and salinity sources of the brine.

2 Regional geology

The Qaidam Basin, located in the northern part of the Tibetan Plateau, is a typical arid interior basin. It is a Cenozoic extensional basin that is surrounded by mountains. The Qilian Mountains, Kunlun Ranges, and Altun Mountains are the basin boundaries on the north, south, and northwest, respectively (Xia et al., 2001; Jolivet et al., 2003; Cowgill, 2007). During the Caledonian, a soft collision intensified the paleo-oceanic trough uplift, followed by an underthrusting period on the northern and southern fringes (Xia et al., 2001). After this period, the Qaidam Basin was limited between the Kunlun and Qilian ranges. In the Mesozoic, there was a series of mantle plume uplift and regional compression, resulting in a structural inverted rift basin in this area (Cheng et al., 2019; Cheng et al., 2021). The embryonic Qaidam Basin was formed by sinistral strike-slip faulting on the Altun Mountains in the late Eocene (Lu and Xiong, 2009). Then, the Altyn Tagh continued to rise and the basin continued to sink, leading to a complete separation between the Qaidam Basin and the Tarim Basin, indicating the formation of the modern Qaidam Basin. After this period, the basin reached a mega-lake environment that evolved into modern salt lakes (Vengosh et al., 1995).

Regarding Xitaijinaier and Dongdabuxun lakes as demarcation points, the Qaidam Basin can be divided into three parts: the eastern, central, and western parts (Figure 1A). The western Qaidam Basin is located between 38° and 39°N and 91° and 93°E, close to the Kunlun mountain fault zone and the Altyn Tagh Fault zone, which is the most intense deformation and tectonic form of the Qaidam Basin.

The Kunteyi Basin is a typical dry sabkha located in the western part of Qaidam and is a crucial potash deposit in China. All intercrystalline brine samples were collected from the central Dayantan Basin, the best ore-forming and largest potash deposit in Kunteyi (Li et al., 2021). It is surrounded by the Eboliang structure in the west, the Hulushan structure in the south, and the Lenghu structure in the east, forming a semi-closed secondary basin. The study area is covered by middle Pleistocene and upper Pleistocene strata, and the old to new strata exposed in the area are the Proterozoic, Ordovician, Devonian, Carboniferous, Jurassic, Tertiary, and Quaternary strata. Four groups of fault structures exist in the region. Three are large in scale, the Shuangqiquan Fault in the west, the remote sensing F_6 Fault in the northeast, and the remote sensing F_5 Fault in the middle of Kunteyi, which may supply the channel for the inflow of hydrothermal water (Figure 1B). Since the beginning of the Archean Luliang Movement, the Dayantan Basin has experienced long-term and complex tectonic movements and has formed well-developed fault blocks and substantial folds (Li et al., 2020). These structures block the surface water supply to the mining area and create conditions for brine formation. The occurrence state of the brine in Kunteyi is mainly the intercrystalline brine, and a small amount of oilfield water is distributed along the eastern Lenghu Fault. The intercrystalline brine in the study area is divided into five layers. Except for the shallow intercrystalline brine distributed in the Holocene series or the upper Pleistocene series, the other four confined aquifers correspond to the Pleistocene salt layer. In this study, we collected the shallow intercrystalline brine and analyzed its hydrochemical and isotopic compositions to explore the evolutionary process of the brine.

3 Method

In this study, 11 samples were collected, including nine intercrystalline brines and two salt lake brines. The sampling point locations are shown in Figure 1C. All the intercrystalline brine samples were collected from the existing engineering boreholes in the mining area 1 m below the water surface.

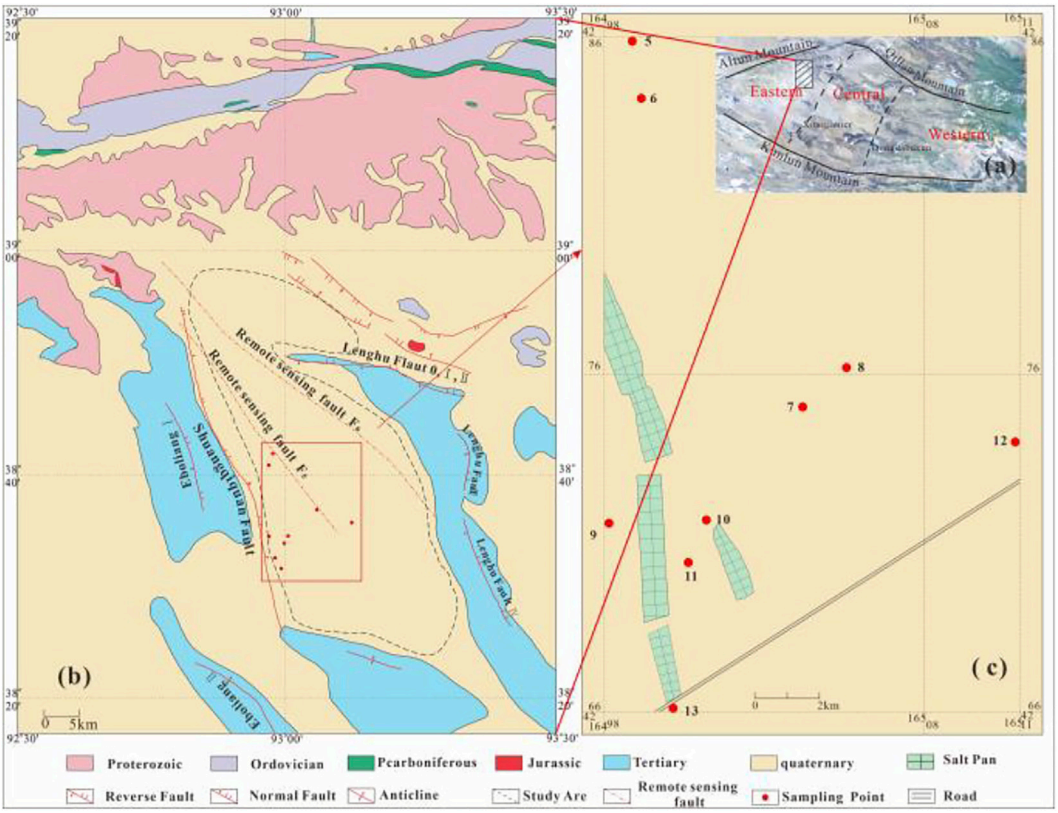

FIGURE 1
(A) Framework of the Qaidam Basin and the location of study area; **(B)** General tectonic features of the study area; **(C)** Location of sampling points.

Therefore, these brine samples belonged to the submersible aquifer. The sample measurements were completed at the analysis and testing center of the Qinghai Institute of Salt Lakes, Chinese Academy of Sciences.

3.1 Element concentration analyses

The concentrations of K^+ and SO_4^{2-} ions and TDS were measured using gravimetric analysis, Ca^{2+} and Mg^{2+} ion concentrations were measured through EDTA titration, Cl^- concentration was measured using $AgNO_3$ titration, and Na^+ ion concentration was assessed *via* subtraction. An inductively coupled plasma emission spectrometer (ICP-MS) was used to analyze the B and Br concentrations. Analytical uncertainties are less than ±5% for B and Br, less than ±2% for Na^+, and less than ±0.5% for all other elements. The results are presented in Table 1.

3.2 Hydrogen and oxygen isotopic analyses

Hydrogen and oxygen isotopic analyses were performed using a stable isotope mass spectrometer (MAT253), and the analytical uncertainties were less than ±0.2% and ±2%, respectively.

3.3 Boron isotopic analysis

The B isotopes were measured at the Chinese Academy of Geological Sciences. The determination process included B purification and isotope determination. In the purification stage, the prepared sample was first diluted with ultrapure water and a solution of low-B boron water, with a B concentration of 10 μg and pH of 6–7. The diluted solutions were passed through a B-specific resin column at a flow rate of 2.5 mL/L for B adsorption. Column elution and B extraction were performed by adding 12 mL of a 0.1 mol/L HCl solution to the resin column at 75°C. The eluent was evaporated and concentrated in a 60-°C purification furnace, and excess ions were removed using an anion and cation-mixed exchange resin column. Then, it was further purified using an eluent without B; the diluted eluents were evaporated, dried at 60°C, and then prepared for isotopic analysis. During the two evaporation processes, mannitol and cesium carbonate (Cs_2CO_3) were added to the eluents to inhibit evaporation.

All B^{11}/B^{10} ratios were determined using a Triton thermal ionization mass spectrometer (Thermo Fisher Company). Our analyses showed a standard deviation of less than 0.2‰ (2σ), as determined by the coeval studies of NIST SRM-951 replicates. Isotope ratios are reported here as a per mil deviation ($\delta^{11}B$) in the B^{11}/B^{10} ratios relative to those of the standard NBS SRM 951:

$$\delta^{11}B(‰) = \left[\left(B^{11}/B^{10}\right)_{sample} / \left(B^{11}/B^{10}\right)_{standard} - 1 \right] \times 1000.$$

TABLE 1 Concentration of major elements, trace elements, hydrogen isotopes, oxygen isotopes, and boron isotopes of brines in the study area.

Sample No.	Type	TDS g/L	K^+ g/L	Na^+ g/L	Mg^{2+} g/L	Ca^{2+} g/L	Cl^- g/L	SO_4^{2-} g/L	HCO_3^- g/L	Br^- mg/L	B mg/L	δ^2H	$\Delta^{18}O$	$\delta^{11}B$	Data source
1	Oilfield brine	43.34	0.25	12.53	0.62	3.61	25.12	0.46	0.69	4.52	55.82	−56.4	−6.5		Li et al. (2019)
2		49.18	0.09	13.18	1.38	3.29	30.85	0.28	0.08	4.77	20.13	−48	0.1		
3		42.43	0.08	11.56	1.09	2.58	26.61	0.06	0.15	19.01	119.5	−39.7	3		
4		33.79	0.07	8.95	1.41	1.88	21.35	0.02	0.09	5.92	11.02	−39.5	3.9		
5	Intercrystalline brine	332.75	4.54	116.44	5.75	0.36	189.59	15.64	0.15	16.98	260	−49	−5.1	21.27	
6		331.75	5.46	113.39	7.05	0.36	189.94	15.06	0.13	13.62	351.5	−47	−4.7	21.67	
7		328.39	2.62	117.37	5.11	0.29	188.21	14.41	0.17	12.78	200.9	−38	−2.6	24.87	
8		328.21	1.66	121.30	2.97	0.44	188.21	13.34	0.18	8.14	110.5	−34	−3.2	21.61	
9		339.32	8.34	96.53	17.69	0.18	186.32	29.88	0.19	9.03	200.9	−33	−2	18.49	
10		344.50	10.43	99.11	15.86	0.44	184.76	33.34	0.32	22.26	221	−39	−4.1	22.58	
11		341.49	10.34	103.39	12.86	0.29	186.66	27.41	0.19	15.16	331.4	−47	−5.1	21.22	
12		331.01	5.50	111.98	7.71	0.36	189.25	15.72	0.17	10.71	301.3	−41	−4	22.37	
13		331.46	6.55	109.78	8.11	0.73	184.59	21.16	0.13	21.23	401.7	−48	−3.3	15.77	
14	Potassium Lake	311.71	3.71	79.22	24.49	2.14	198.56	3.05	0.22	8.34	301.3	−30	1.8	9.25	
20	Sugan Lake	68.37	0.33	20.26	1.00	0.04	0.47	46.10	0.17	4.23	15.06	−69	−9.4	5.27	
21	Seawater	32.00	0.34	9.89	1.19	0.38	17.53	2.42	0.13	61	4.3	0	0		Chen (1983)

10.3389/fenvs.2023.1106181

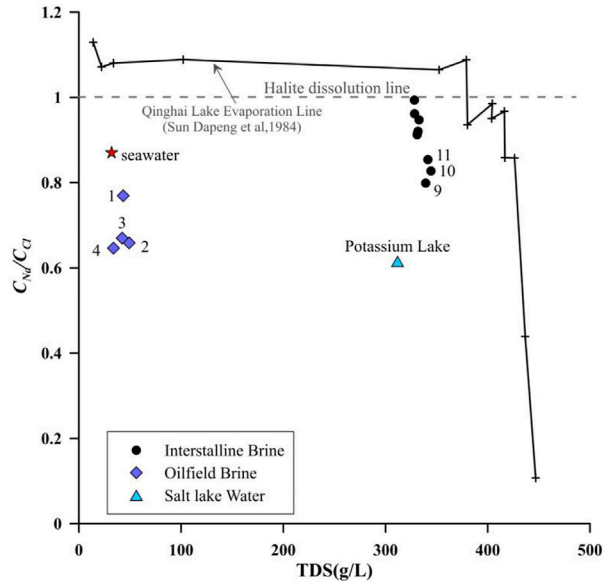

FIGURE 2
Comparative C_{Na}/C_{Cl} ratio distribution and total dissolved solids (TDS) of the intercrystalline brine, oilfield brine, and salt lake water.

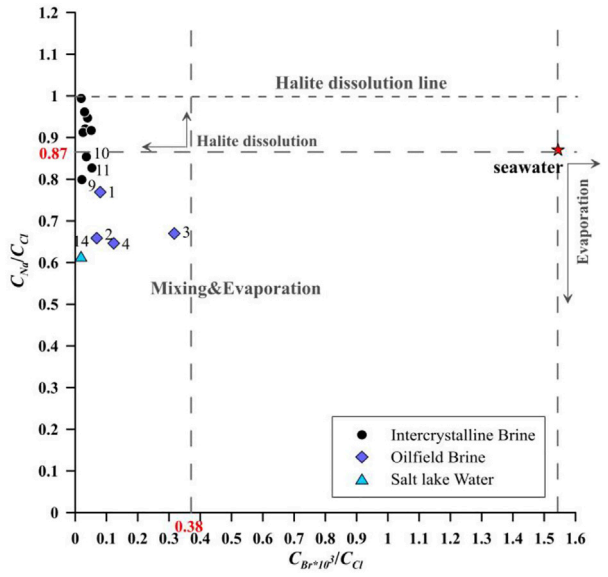

FIGURE 3
Relationship between the C_{Na}/C_{Cl} ratio and C_{Br}/C_{Cl} ratio of the intercrystalline brine, oilfield brine, and salt lake water. Data for oilfield brine are extracted from Li et al. (2019).

The mean of the absolute B^{11}/B^{10} ratios of NIST SRM-951 replicates analyzed alongside the samples was 4.05262 ± 0.00077 (2σ = 0.02%; n = 9).

4 Results

The chemical and isotopic compositions of the samples in the study area are listed in Table 1. The data on the intercrystalline brine and salt lake brine were measured in this study. Data from seawater and the oilfield brine of the Kunteyi Salt Lake, reported by Chen (1983) and Li et al. (2019), were selected as a comparison (Table 1) to understand the formation process of the brine.

4.1 Water chemistry

The average value of TDS in the intercrystalline brine of Kunteyi is 334.04 g/L. It is almost ten times higher than the TDS value of seawater and the oilfield brine from Kunteyi but is similar to the TDS value of the brine from the oilfield of northern Qaidam (Tan et al., 2011). The major anions and cations of the brine in Kunteyi are Cl^- (184,589.9–198,563.5 mg/L) and Na^+ (96,527.64–121,296.22 mg/L) ions, respectively, which together account for 90% of TDS. Compared with the oilfield brine, the intercrystalline brine has a much higher K^+ and SO_4^{2-} concentration, indicating a possible influence of the evaporation stage of halite sedimentation (Liu et al., 2016). According to the sequence of mineral precipitation in Qinghai Lake evaporated during the experiment given by Sun et al. (2002), the K^+ and SO_4^{2-} concentrations continued to increase until the end of evaporation. However, the Cl^- concentration in the intercrystalline brine was much higher than that in the residual solution after halite deposition. The brine of the Potassium Lake, located near the study area, is rich in Mg^{2+}, Ca^{2+}, and Cl^-. These

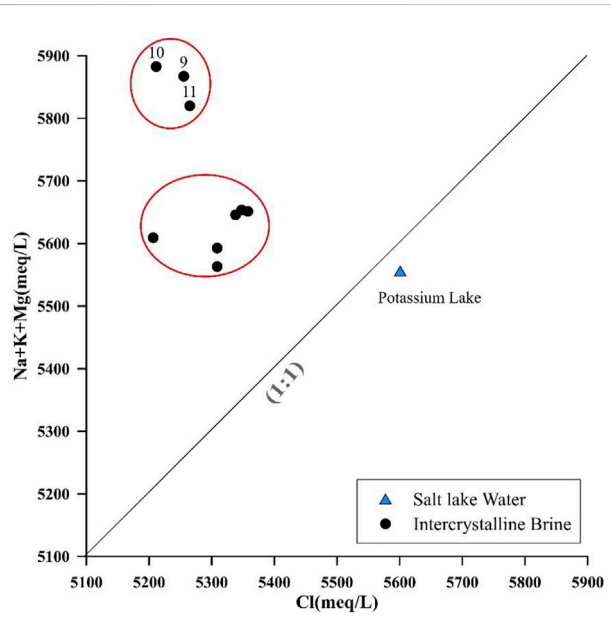

FIGURE 4
Relationship between (Na + K + Mg) and Cl in intercrystalline brines and salt lake water in the study area.

phenomena indicate that the evolution of the brine may be simultaneously controlled by evaporation and influenced by the Ca–Cl-type water.

Boron and bromine are ideal elements for identifying the origin of the salinity. Therefore, the concentrations of these two elements were tested in this study. The results show that the Br concentration of the intercrystalline brine ranges from 8.14 to 22.26 mg/L, considerably lower than the initial Br concentration of seawater caused by

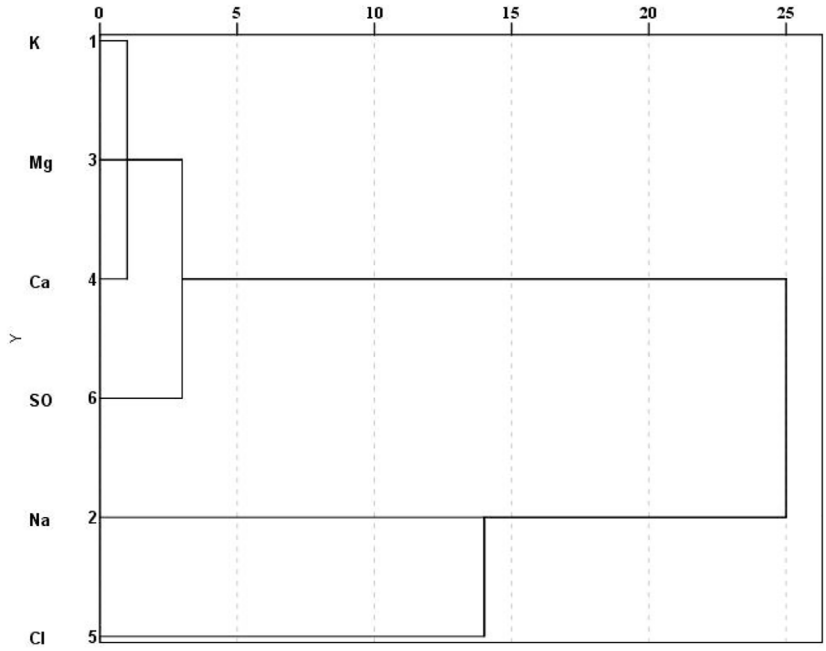

FIGURE 5
Cluster analysis of the major ions of the intercrystalline brine.

evaporation. The concentration of B ranges from 110.50 to 401.70 mg/L, while the concentration of B in seawater is only 4.30 mg/L (Chen, 1983). These results indicate that the intercrystalline brine of Kunteyi is of non-marine origin.

4.2 Isotopic ratios of the intercrystalline brine

It can be seen from Table 1 that the characteristics of the H, O, and B isotopic compositions are considerably different between brine, oilfield water, and salt lake water. The δ^2H and $\delta^{18}O$ values of the intercrystalline brine range from −49 to −33‰ (average −41.7‰) and from −5.1 to −2.0‰ (average −3.8‰), respectively. The oilfield water has a positive $\delta^{18}O$ value, with an average 0.12‰, and a similar δ^2H, with an average −45.9‰, which may indicate that the intercrystalline brine underwent a more intense evaporation process than the oilfield water.

As B isotopes do not react with other elements during the water cycle, these often are used to distinguish the different sources of salinity, such as eluviation and ancient brine precipitation (Fan et al., 2010). In this study, the average $\delta^{11}B$ value of the intercrystalline brine is 21.09‰, whereas that of the Potassium Lake is 9.26‰.

5 Discussion

5.1 Chemical evolution of the brine

The ratios of the chemical compositions are valuable tools for tracing the sources of brine salinity and its evolution. The relationship between the molar concentration ratio C_{Na}/C_{Cl} and TDS can reveal the salinity enrichment process (Engle and Rowan, 2013). During evaporation, the TDS of the solution increased continuously (Ye et al., 2015). The oilfield brine is far from the evaporation line and halite dissolution line and instead has a similar C_{Na}/C_{Cl} ratio to that of seawater, as shown in Figure 2. In contrast to the oilfield brine, the C_{Na}/C_{Cl} ratio of the intercrystalline brine in this study showed a similar trend to that of the Qinghai Lake evaporation line but had a lower TDS concentration, suggesting that evaporation is the main factor in the formation of the intercrystalline brine but not the only factor. The lower TDS concentration is likely caused due to the simultaneous freshwater intrusion. Halite dissolution is another crucial process that results in Na^+ enrichment, maintaining a C_{Na}/C_{Cl} ratio of approximately 1 (Han et al., 2014; Llewellyn, 2014). However, the C_{Na}/C_{Cl} ratio of all the samples was less than 1, and the minimum value of the intercrystalline brine is 0.79. The processes that can cause this phenomenon include cation exchange and absorption, mixing of Ca–Cl water, and dissolution of other Cl-containing minerals (Liu et al., 2016). Therefore, the C_{Na}/C_{Cl} ratio alone cannot clearly explain the origin of the salinity.

Like other halogens, bromide exists in nature only in an oxidation state (Gupta et al., 2012). The chemical properties of Br^- are relatively conservative, and Br^- is not easily absorbed by coprecipitation. In the process of seawater evaporation, the concentration of Br^- increases because it is difficult for Br^- to enter the crystal lattice of halite and coprecipitate with it (Liu et al., 2016). In contrast, brines formed by the dissolution of non-marine evaporites had a much smaller content of Br^-. Therefore, the C_{Br}/C_{Cl} ratio commonly helps in identifying the source of salts during the leaching of halite and other minerals (Li et al., 2015). Figure 3 plots the relationship between the C_{Na}/C_{Cl} ratio and C_{Br}/C_{Cl} ratio to analyze the evolution process of the brine. The seawater had C_{Na}/C_{Cl} = 0.87 and C_{Br}/C_{Cl} = 1.54. With evaporation, Na^+ and Cl^- were precipitated continuously with the increasing Br^- concentration. Therefore, the sedimentary brine usually shows $C_{Na}/$

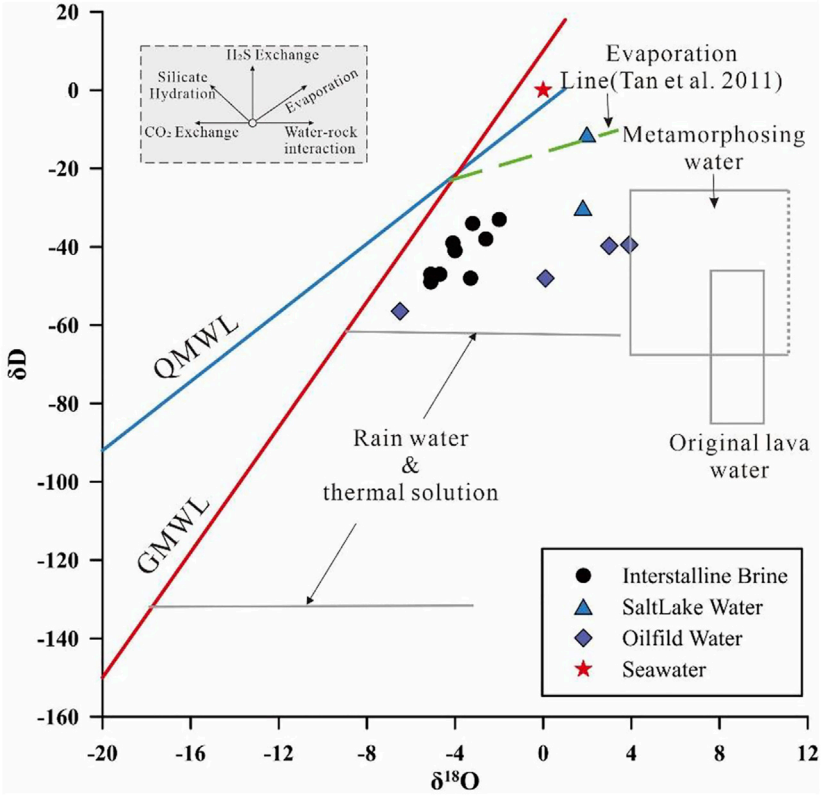

FIGURE 6
Relationship between δ^2H and $\delta^{18}O$ of the intercrystalline brine, oilfield brine, and salt lake water. Data for the oilfield brine are extracted from Li et al. (2019).

C_{Cl} <0.87 and C_{Br}/C_{Cl} >1.54. For the halite dissolution brine, the C_{Na}/C_{Cl} ratio is higher than 0.87 and the C_{Br}/C_{Cl} ratio is smaller than 0.38 (Li et al., 2013a). The characteristic coefficients of most intercrystalline brines conform to the process of halite dissolution, as shown in Figure 3. However, points 9 to 11 have C_{Na}/C_{Cl} ratios less than 0.87 and C_{Br}/C_{Cl} ratios less than 0.38, which plot in the same area as the oilfield brine. The oilfield brine of Kunteyi is affected by a Ca–Cl-type hydrothermal fluid (Li et al., 2019). This process may increase Ca^{2+} simultaneously, but the intercrystalline brine in this area has a low Ca^{2+} content. Two possible modes of evolution may lead to an increase in the concentration of Cl^- ions accompanied by a low Ca^{2+} ion concentration. In the first mode, the Ca–Cl-type water intrudes into the study area, and Ca^{2+} ions react with CO_3^{2-} ions and deposit, whereas the second mode may involve the dissolution of other Cl-bearing minerals, such as sylvine.

The dissolution of Cl-bearing minerals would elevate the Cl^- concentration and give a Cl/(Na + K + Mg) ratio of approximately 1 in groundwater. However, this ratio of the intercrystalline brine plot is scattered, and all points are above the 1:1 line (Figure 4). These samples can be divided into two groups, and points 9, 10, and 11 have significantly higher (Na + K + Mg) concentrations, proving that there may be other mineral dissolution processes providing more cations without chlorine to the intercrystalline brine.

Cluster analysis divides the data on unknown categories into different classes or clusters through statistical methods and then identifies the data changed with the same rule. This method has been used widely to classify groundwater and identify groundwater flow and geochemical processes (Lyu et al., 2019). Cluster analysis was used on the major ion concentration of all intercrystalline brines in the study area to find the similarity of different ion concentration variation trends and identify which mineral participates in the dissolution quickly. The cluster analysis results are presented as a dendrogram (Figure 5). In this study, the ions were divided into two groups. One group included Na^+ and Cl^-, which resulted in the dissolution of the halite. This result was obtained by analyzing the C_{Na}/C_{Cl} and C_{Br}/C_{Cl} ratios. The other group includes K^+, Ca^{2+}, Mg^{2+}, and SO_4^{2-}, which are contained in polyhalite ($K_2Ca_2Mg\ [SO_4]_4{\cdot}2H_2O$). A large amount of polyhalite is buried in the Pleistocene strata of Kunteyi. However, this mineral is difficult to develop because of its insoluble characteristics and deeply buried layers (Yuan et al., 2021). All brines analyzed in this study were collected during the Holocene, and it needs to be further confirmed whether polyhalite buried in the Pleistocene can influence K^+ and Mg^{2+} concentrations in the superficial layer. There are three deep faults, F_5, F_6, and Shuangqiquan faults, located in the middle and western boundaries of Kunteyi. They provide a channel for deep water to recharge the shallow brine. Most hydrothermally, Ca–Cl brines are known to dissolve polyhalite effectively (Li et al., 2020). Therefore, in the process of brine evolution, Cl^--containing water from the deep layer may have been trapped in the Pleistocene and may have dissolved the polyhalite in this layer. The solution was then replenished upward along the deep faults and flowed into the Holocene, improving the K^+ and Mg^{2+}

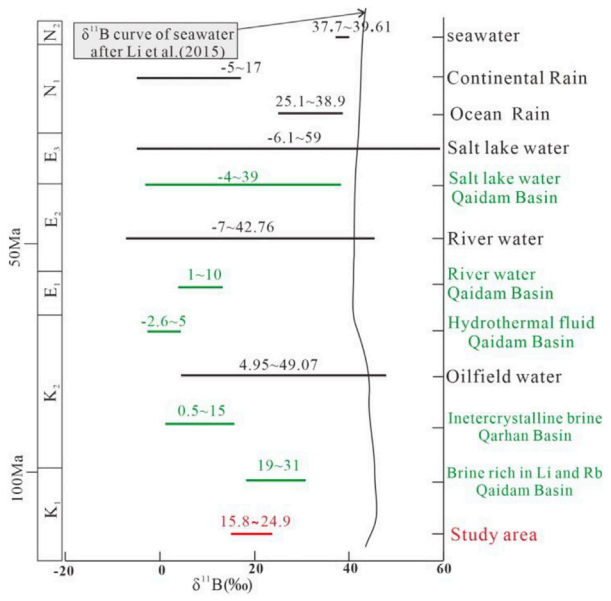

FIGURE 7
Comparison of $\delta^{11}B$ values of different solutions. The salt lake water data in the Qaidam Basin are extracted from Xiao et al. (1999), the river water data in the Qaidam Basin are extracted from Hussain et al. (2021), the oilfield water data are extracted from Li et al. (2013b), the intercrystalline brine data in the Qarhan Basin are extracted from Fan et al. (2015), and the data on the brine rich in Li and Rb in the Qarhan Basin are extracted from Li et al. (2022).

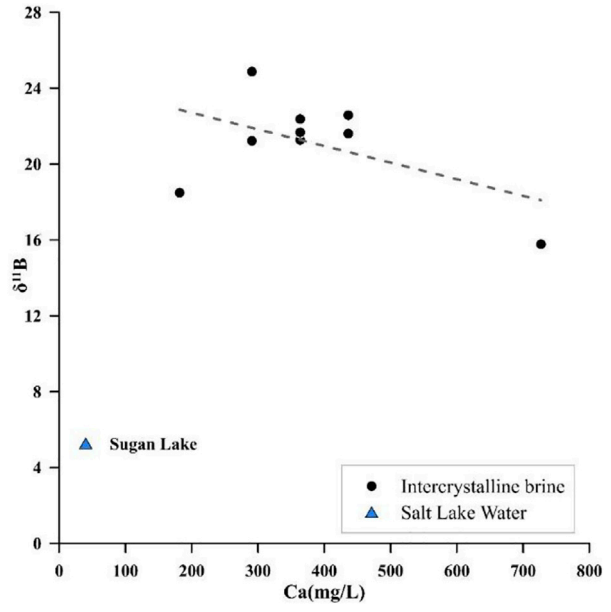

FIGURE 8
Relationship between $\delta^{11}B$ values and the Ca content of the intercrystalline brine and salt lake water.

concentrations of the intercrystalline brine. Simultaneously, the high concentration of Cl^- in the solution inhibited halite dissolution and led to a C_{Na}/C_{Cl} ratio smaller than 1.

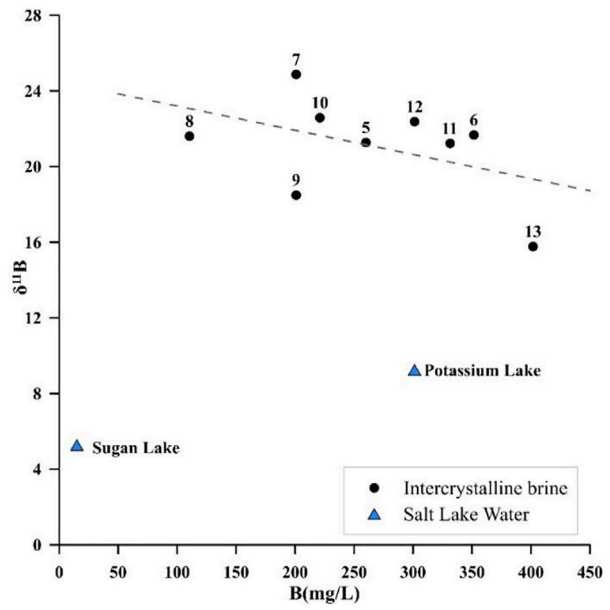

FIGURE 9
Relationship between $\delta^{11}B$ values and the B content of the intercrystalline brine and salt lake water.

From the aforementioned analysis, points 9, 10, and 11 (Figure 4) showed many different hydrochemical characteristics compared to the other points. The brine sampled from these three points has a lower C_{Na}/C_{Cl} ratio and Cl/(Na + K + Mg) ratio because the brine is rich in K^+ and Mg^{2+} and poor in Na^+. These three points are located near the Shuangqiquan Fault and may receive more polyhalite dissolution water containing high K^+ and Mg^{2+} ion concentrations than polyhalite water received by other intercrystalline brine points.

5.2 Hydrogen and oxygen isotopes

The isotopes δ^2H and $\delta^{18}O$ are good conservative tracers for identifying recharge sources because they are the part of the water molecule itself, which can reflect its history and origin before infiltration (Clark and Fritz, 2013). The $\delta^{18}O$ isotopes of intercrystalline brines are relatively lighter, ranging from −5.1 to −2‰, compared to those of the oilfield brines of Kunteyi, and almost similar δ^2H isotopes, ranging from −49 to −33‰. As Figure 6 shows, all the isotopic data lie on the right of the Global Meteoric Water Line (GMWL, $\delta^2H = 8 \times \delta^{18}O - 46$) and Qaidam Meteoric Water Line (QMWL, $\delta^2H = 4.4 \times \delta^{18}O - 4.0$) in the plot of δ^2H vs. $\delta^{18}O$ (Craig, 1961; Fan et al., 2010). The apparent positive shift in $\delta^{18}O$ may be caused by water–rock interactions (Cartwright et al., 2004; Boschetti et al., 2020). The equation of the fitting curve for the intercrystalline brine ($\delta^2H = 4.3 \times \delta^{18}O - 25$) is almost parallel to the QMWL, indicating an atmospheric water origin of the water source of the intercrystalline brine. However, owing to the evaporation effect, the light isotope (H) migrates to the gas phase, whereas the heavy isotope (D) tends to be enriched in the weakly active phase and retained in the original brine solution. Thus, the surface brine has a heavier δ^2H value than the δ^2H values of all intercrystalline plots below the evaporation line. Evaporation is not a primary process

in brine evolution. The oilfield brine will have frequent water–rock interactions, leading to a much heavier $\delta^{18}O$ value, owing to the enclosed space compared to that of the intercrystalline brine. Notably, the oilfield water in the study area is close to the hydrothermal distribution area (Figure 6). The oilfield brine of Kunteyi has been proven to be affected by deep hydrothermal water influxes (Tan et al., 2011), and therefore, the comparatively lighter $\delta^{2}H$ of the intercrystalline brine may also be caused by the inflow of hydrothermal water, which has a negative $\delta^{2}H$ value. Simultaneously, the positive $\delta^{18}O$ value may have been influenced by the water–rock interaction and evaporation, consistent with the conclusions obtained from the chemical analyses.

5.3 Boron isotopes

Natural boron exists as either tetrahedral (i.e., $B(OH)_3$) or trigonal complexes (i.e., $B(OH)_4^-$) (Barth, 1993). Differences in their reduced partition function ratios and relative masses result in two stable isotopes, B^{11} and B^{10}, showing significant isotopic fractionation (Ren et al., 2018), leading to considerable variations in natural $\delta^{11}B$ (Figure 7). Thus, boron isotopes can readily distinguish the evolution of brines. All the intercrystalline brine samples exhibited $\delta^{11}B$ values of 15.77‰–25.87‰, with an average value of 21.1‰. These values are considerably higher than those of the intercrystalline brine from the Qarhan Basin and similar to those of brines rich in Li and Rb, identified to be influenced by thermal water, as shown in Figure 7. Compared with the brine from the Potassium Lake and Sugan Lake (values 9.25‰ and 5.27‰), which represent the $\delta^{11}B$ value of the residual brine of evaporation, the $\delta^{11}B$ values of the intercrystalline brine are much higher. During the evaporation of seawater, $\delta^{11}B$ values will increase with an increase in the water concentration (Kloppmann et al., 2001). However, in non-marine evaporation environments with a pH less than 7, $\delta^{11}B$ values change oppositely, indicating that the high $\delta^{11}B$ value of the intercrystalline brine is not due to evaporation (Yingkai and Lan, 2001). Another process that occurred in the study area is halite dissolution. According to Qin et al. (2021), B ions would not enter the crystal lattice during halite deposition and without isotopic fractionation; therefore, halite dissolution does not affect $\delta^{11}B$ of brines.

Two reactions can lead to the $\delta^{11}B$ increase, clay absorption, and hydrothermal recharge (Hemming and Hanson, 1992). When clay absorption occurs, the Na^+ and K^+ concentrations decrease in contrast to the hydrochemical analysis, which indicated that no clay absorption occurred in the study area. The hydrothermal process is Ca–Cl-type water with a low $\delta^{11}B$ value. It can react with CO_3^{2-} ions and make $B(OH)_4^-$ ions, enrich with B^{10}, and coprecipitate with $CaCO_3$, and this process will decrease B and Ca^{2+} concentrations and increase the $\delta^{11}B$ value (Xiao et al., 1999). There is no significant correlation between Ca vs. $\delta^{11}B$ and B vs. $\delta^{11}B$, and the *p*-value of these two groups is higher than 0.05, as shown in Figures 8, 9. However, the number of samples was insufficient to reflect the statistical law. However, the fit line showed a downward trend. Compared with Potassium Lake water, the intercrystalline brine has larger $\delta^{11}B$ isotope values and lower Ca^{2+} concentrations. Both of these phenomena can effectively confirm the influence of hydrothermal treatment.

5.4 Origin of the intercrystalline brine

Synthesizing the previous results inferred from multiple chemical and isotopic analyses with geological structures and hydrogeological conditions, a conceptual model for the origin of saline and brine groundwater in shallow aquifers can be inferred. The shallow intercrystalline brine in the Holocene is modern, and the water source is mainly atmospheric precipitation. Atmospheric water with a low TDS value is stored in the formation, which dissolves a large amount of halite and increases the concentration of Na^+ and Cl^- ions in the solution. Simultaneously, the brine in the deep formation of the Pleistocene was affected by the Ca–Cl-type deep hydrothermal water, and polyhalite dissolution and $CaCO_3$ precipitation occurred to form Mg- and K-rich ionic brines. The brine rose along the channel formed by the fracture and was supplied to the shallow intercrystalline brine.

6 Conclusion

The chemical characteristics and isotopic compositions of the intercrystalline brine in Kunteyi display a non-marine origin, and they are influenced by mineral dissolution, geothermal system heat sources, and water recharge sources.

(1) From the perspective of H and O isotopic compositions, the fitting curve of the H and O isotope values of the intercrystalline brine is almost parallel to the local meteoric water line, and there is an apparent O isotope positive drift, indicating that the water source in this area is mainly atmospheric water.
(2) The curves of C_{Na}/C_{Cl} vs. TDS and C_{Na}/C_{Cl} vs. C_{Br}/C_{Cl} show that halite is the main dissolved mineral in the formation and is also the primary source of salinity in the brine. However, the high content of Mg^{2+} and K^+ ions, and the ion cluster analysis showed that polyhalite dissolution is another source of salinity for the brine.
(3) The analyses of the C_{Br}/C_{Cl} ratio and $\delta^{11}B$ show that the study area was affected by the hydrothermal fluid. The hydrothermal fluid first stranded in the Pleistocene dissolved polyhalite and continued to recharge the shallow intercrystalline brine such that K^+ ions in the brine increased to the mining grade.

Data availability statement

The original contributions presented in the study are included in the article/Supplementary Materials; further inquiries can be directed to the corresponding author.

Author contributions

QR: methodology, analysis, visualization, validation, and writing—original draft. BL: sampling, data test, and supervision. YZ: investigation and writing—review and editing. HW: investigation and writing—review and editing.

Funding

This research work is supported by the National Key Laboratory Opening Fund Project of Hydroscience and Engineering—Tsinghua University (No. sklhse-2020-B-04).

Acknowledgments

The authors would like to thank all the workers who assisted with analyzing boron isotope contents. They all acknowledge the Frontier Editorial Team for their professional handling of the manuscript and dedicated referees who provided very constructive and insightful comments to significantly improve the quality of the work.

Conflict of interest

The authors declare that the research was conducted in the absence of any commercial or financial relationships that could be construed as a potential conflict of interest.

Publisher's note

References

Bagheri, R., Nadri, A., Raeisi, E., Kazemi, G., Eggenkamp, H., and Montaseri, A. (2014). Origin of brine in the kangan gasfield: Isotopic and hydrogeochemical approaches. *Environ. Earth Sci.* 72 (4), 1055–1072. doi:10.1007/s12665-013-3022-7

Barth, S. (1993). Boron isotope variations in nature: A synthesis. *Geol. Rundsch.* 82 (4), 640–651. doi:10.1007/bf00191491

Basyoni, M. H., and Aref, M. A. (2016). Composition and origin of the sabkha brines, and their environmental impact on infrastructure in Jizan area, Red Sea Coast, Saudi Arabia. *Environ. Earth Sci.* 75 (2), 105–117. doi:10.1007/s12665-015-4913-6

Bershaw, J., Penny, S. M., and Garzione, C. N. (2012). Stable isotopes of modern water across the Himalaya and eastern Tibetan Plateau: Implications for estimates of paleoelevation and paleoclimate. *J. Geophys. Res. Atmos.* 117 (D2), 16132. doi:10.1029/2011JD016132

Boschetti, T., Awadh, S. M., Al-Mimar, H. S., Iacumin, P., Toscani, L., Selmo, E., et al. (2020). Chemical and isotope composition of the oilfield brines from Mishrif Formation (southern Iraq): Diagenesis and geothermometry. *Mar. Petroleum Geol.* 122, 104637. doi:10.1016/j.marpetgeo.2020.104637

Cartwright, I., Weaver, T. R., Fulton, S., Nichol, C., Reid, M., and Cheng, X. (2004). Hydrogeochemical and isotopic constraints on the origins of dryland salinity, Murray Basin, Victoria, Australia. *Appl. Geochem.* 19 (8), 1233–1254. doi:10.1016/j.apgeochem.2003.12.006

Chen, Y. (1983). Sequence of salt separation and regularity of some trace elements distribution during isothermal evaporation (25 °C) of the Huanghai seawater. *Acta Geol. Sin.* 4, 379–390.

Cheng, F., Garzione, C. N., Jolivet, M., Guo, Z., Zhang, D., Zhang, C., et al. (2019). Initial deformation of the northern Tibetan plateau: Insights from deposition of the lulehe formation in the Qaidam Basin. *Tectonics* 38 (2), 741–766. doi:10.1029/2018TC005214

Cheng, F., Jolivet, M., Guo, Z., Wang, L., Zhang, C., and Li, X. (2021). Cenozoic evolution of the Qaidam Basin and implications for the growth of the northern Tibetan plateau: A review. *Earth-Science Rev.* 220, 103730. doi:10.1016/j.earscirev.2021.103730

Clark, I. D., and Fritz, P. (2013). *Environmental isotopes in hydrogeology*. Lewis, Boca Raton: CRC Press.

Cowgill, E. (2007). Impact of riser reconstructions on estimation of secular variation in rates of strike–slip faulting: Revisiting the Cherchen River site along the Altyn Tagh Fault, NW China. *Earth Planet. Sci. Lett.* 254 (3-4), 239–255. doi:10.1016/j.epsl.2006.09.015

Craig, H. (1961). Isotopic variations in meteoric waters. *Science* 133 (3465), 1702–1703. doi:10.1126/science.133.3465.1702

Du, Y., Ma, T., Chen, L., Xiao, C., and Liu, C. (2016). Chlorine isotopic constraint on contrastive Genesis of representative coastal and inland shallow brine in China. *J. Geochem. Explor.* 170, 21–29. doi:10.1016/j.gexplo.2016.07.024

Engle, M. A., and Rowan, E. L. (2013). Interpretation of Na–Cl–Br systematics in sedimentary basin brines: Comparison of concentration, element ratio, and isometric log-ratio approaches. *Math. Geosci.* 45 (1), 87–101. doi:10.1007/s11004-012-9436-z

Fan, Q., Ma, H., Lai, Z., Tan, H., and Li, T. (2010). Origin and evolution of oilfield brines from Tertiary strata in Western Qaidam Basin: Constraints from 87Sr/86Sr, δD, δ18O, δ34S and water chemistry. *Chin. J. Geochem.* 29 (4), 446–454. doi:10.1007/s11631-010-0478-y

Fan, Q., Ma, Y., Cheng, H., Wei, H., Yuan, Q., Qin, Z., et al. (2015). Boron occurrence in halite and boron isotope geochemistry of halite in the Qarhan Salt Lake, Western China. *Sediment. Geol.* 322, 34–42. doi:10.1016/j.sedgeo.2015.03.012

Farber, E., Vengosh, A., Gavrieli, I., Marie, A., Bullen, T. D., Mayer, B., et al. (2007). The geochemistry of groundwater resources in the Jordan valley: The impact of the rift valley brines. *Appl. Geochem.* 22 (3), 494–514. doi:10.1016/j.apgeochem.2006.12.002

Gupta, I., Wilson, A. M., and Rostron, B. J. (2012). Cl/Br compositions as indicators of the origin of brines: Hydrogeologic simulations of the Alberta Basin, Canada. *Bulletin* 124 (1-2), 200–212. doi:10.1130/B30252.1

Han, D., Song, X., Currell, M. J., Yang, J., and Xiao, G. (2014). Chemical and isotopic constraints on evolution of groundwater salinization in the coastal plain aquifer of Laizhou Bay, China. *J. Hydrology* 508, 12–27. doi:10.1016/j.jhydrol.2013.10.040

Han, J., Zhou, X., Jiang, C., Hu, L., Fang, B., and Sun, Q. (2013). Hydrochemical characteristics, origin and evolution of the subsurface brines in western Qaidam Basin. *GEOSCIENCE* 27 (6), 1454–1464.

Hemming, N. G., and Hanson, G. N. (1992). Boron isotopic composition and concentration in modern marine carbonates. *Geochimica Cosmochimica Acta* 56 (1), 537–543. doi:10.1016/0016-7037(92)90151-8

Hussain, S. A., Han, F.-Q., Ma, Z., Hussain, A., Mughal, M. S., Han, J., et al. (2021). Unraveling sources and climate conditions prevailing during the deposition of neoproterozoic evaporites using coupled chemistry and boron isotope compositions (δ11B): The example of the salt range, Punjab, Pakistan. *Minerals* 11 (2), 161. doi:10.3390/min11020161

Jolivet, M., Brunel, M., Seward, D., Xu, Z., Yang, J., Malavieille, J., et al. (2003). Neogene extension and volcanism in the Kunlun fault zone, northern tibet: New constraints on the age of the Kunlun fault. *Tectonics* 22 (5), 1428. doi:10.1029/2002TC001428

Kloppmann, W., Négrel, P., Casanova, J., Klinge, H., Schelkes, K., and Guerrot, C. (2001). Halite dissolution derived brines in the vicinity of a Permian salt dome (N German Basin). Evidence from boron, strontium, oxygen, and hydrogen isotopes. *Geochimica Cosmochimica Acta* 65 (22), 4087–4101. doi:10.1016/S0016-7037(01)00640-8

Li, C., Chen, X., Guo, H., Zhou, X., and Cao, J. (2021). Production of potash and N-Mg compound fertilizer via mineral shoenite from Kunteyi Salt Lake: Phase diagrams of quaternary system (NH4) 2SO4-MgSO4-K2SO4-H2O in the isothermal evaporation and crystallization process. *Acta Geol. Sinica-English Ed.* 95 (3), 1016–1023. doi:10.1111/1755-6724.14409

Li, J., Li, T., Ma, H., and Peng, X. (2013a). Investigation of the chemical characteristics and its geological significance of the Tertiary oilfield brine in the Western Qaidam basin. *HYDROGEOLOGY Eng. Geol.* 40 (6), 28–36.

Li, J., Li, T., Ma, Y., and Chen, F. (2022). Distribution and origin of brine-type Li-Rb mineralization in the Qaidam Basin, NW China. *Sci. China Earth Sci.* 65 (3), 477–489. doi:10.1007/s11430-021-9855-6

Li, M. H., Yan, M. D., Wang, Z. R., Liu, X. M., Fang, X. M., and Li, J. (2015). The origins of the mengye potash deposit in the lanping–simao basin, yunnan province, western China. *OreGeology Rev.* 69, 174–186. doi:10.1016/j.oregeorev.2015.02.003

Li, R., Liu, C., Jiao, P., Liu, W., Tang, D., and Wang, S. (2020). The effect of solvent chemistry on potassium dissolution extraction from low-grade solid potash ore in Qarhan Salt Lake, China. *Appl. Geochem.* 115, 104550. doi:10.1016/j.apgeochem.2020.104550

Li, T., Li, J., Ma, H., and Li, B. (2013b). Boron isotope geochemical study on oil-field brine in western Qaidam Basin. *J. Salt Lake Reserch* 21 (2), 1–9.

Li, Y., Li, J., Fan, Q., Wang, M., and Shan, F. (2019). Origin of deep intercrystalline brines from dayantan mine area in Qaidam Basin. *J. Salt Lake Reserch* 27 (1), 82–88.

Liu, J., Chen, Z., Wang, L., Zhang, Y., Li, Z., Xu, J., et al. (2016). Chemical and isotopic constrains on the origin of brine and saline groundwater in Hetao plain, Inner Mongolia. *Environ. Sci. Pollut. Res.* 23 (15), 15003–15014. doi:10.1007/s11356-016-6617-1

Llewellyn, G. T. (2014). Evidence and mechanisms for Appalachian Basin brine migration into shallow aquifers in NE Pennsylvania, USA. *Hydrogeology J.* 22 (5), 1055–1066. doi:10.1007/s10040-014-1125-1

Lu, H., and Xiong, S. (2009). Magnetostratigraphy of the dahonggou section, northern Qaidam Basin and its bearing on cenozoic tectonic evolution of the qilian Shan and Altyn Tagh fault. *Earth Planet. Sci. Lett.* 288 (3-4), 539–550. doi:10.1016/j.epsl.2009.10.016

Lyu, M., Pang, Z., Huang, T., and Yin, L. (2019). Hydrogeochemical evolution and groundwater quality assessment in the dake lake basin, northwest China. *J. Radioanalytical Nucl. Chem.* 320 (3), 865–883. doi:10.1007/s10967-019-06515-8

Qin, X., Ma, H., Zhang, X., Hu, X., Li, G., Jiang, Z., et al. (2021). Origin and evolution of saline spring water in north and Central Laos based on hydrochemistry and stable isotopes (δD, δ18O, δ11B, and δ37Cl). *Water* 13 (24), 3568. doi:10.3390/w13243568

Ren, Q., Du, Y., Gao, D., Lii, B., Zhang, X., Liu, X., et al. (2018). A multi–fluid constrain for the forming of potash deposits in the savannakhet basin: Geochemical evidence from halite. *Acta Geol. Sinica-English Ed.* 92 (2), 755–768. doi:10.1111/1755-6724.13552

Royden, L. H., Burchfiel, B. C., and van der Hilst, R. D. (2008). The geological evolution of the Tibetan Plateau. *Science* 321 (5892), 1054–1058. doi:10.1126/science.1155371

Sun, D., Li, B., Ma, Y., and Liu, Q. (2002). An investigation on evaporating experiments for Qinghai Lake water, China. *J. Salt Lake Res.* 10 (4), 1–12. doi:10.3969/j.issn.1008-858X.2002.04.001

Tan, H., Rao, W., Ma, H., Chen, J., and Li, T. (2011). Hydrogen, oxygen, helium and strontium isotopic constraints on the formation of oilfield waters in the Western Qaidam Basin, China. *J. Asian Earth Sci.* 40 (2), 651–660. doi:10.1016/j.jseaes.2010.10.018

Tapponnier, P., Zhiqin, X., Roger, F., Meyer, B., Arnaud, N., Wittlinger, G., et al. (2001). Oblique stepwise rise and growth of the Tibet Plateau. *Science* 294 (5547), 1671–1677. doi:10.1126/science.105978

Vengosh, A., Chivas, A., Starinsky, A., Kolodny, Y., Baozhen, Z., and Pengxi, Z. (1995). Chemical and boron isotope compositions of non-marine brines from the Qaidam Basin, Qinghai, China. *Chem. Geol.* 120 (1-2), 135–154. doi:10.1016/0009-2541(94)00118-R

Xia, W., Zhang, N., Yuan, X., Fan, L., and Zhang, B. (2001). Cenozoic Qaidam Basin, China: A stronger tectonic inversed, extensional rifted basin. *AAPG Bull.* 85 (4), 715–736. doi:10.1306/8626c98d-173b-11d7-8645000102c1865d

Xiao, Y., Liu, W., Wang, W., and Jin, L. (1999). Boron isotope geochemistry of salt lakes in Qaidam Basin, Qinghai. *Adv. Nat. Sci.* 9 (7), 616–618.

Ye, C., Zheng, M., Wang, Z., Hao, W., Wang, J., Lin, X., et al. (2015). Hydrochemical characteristics and sources of brines in the Gasikule salt lake, Northwest Qaidam Basin, China. *Geochem. J.* 49 (5), 481–494. doi:10.2343/geochemj.2.0372

Yin, A., and Harrison, T. M. (2000). Geologic evolution of the Himalayan-Tibetan orogen. *Annu. Rev. Earth Planet. Sci.* 28 (1), 211–280. doi:10.1146/annurev.earth.28.1.211

Yingkai, X., and Lan, W. (2001). The effect of pH and temperature on the isotopic fractionation of boron between saline brine and sediments. *Chem. Geol.* 171 (3-4), 253–261. doi:10.1016/S0009-2541(00)00251-5

Yu, J., Gao, C., Cheng, A., Liu, Y., Zhang, L., and He, X. (2013). Geomorphic, hydroclimatic and hydrothermal controls on the formation of lithium brine deposits in the Qaidam Basin, northern Tibetan Plateau, China. *Ore Geol. Rev.* 50, 171–183. doi:10.1016/j.oregeorev.2012.11.001

Yuan, X., Meng, F., Zhang, X., Sheng, J., Galamay, A., Cheng, H., et al. (2021). Ore-forming fluid evolution of shallow polyhalite deposits in the Kunteyi playa in the north Qaidam Basin. *Front. Earth Sci.* 727, 698347. doi:10.3389/feart.2021.698347